PCCP

Photophysics and Charge Transfer in Oligo(thiophene) Based Conjugated Diblock Oligomers

Journal:	*Physical Chemistry Chemical Physics*
Manuscript ID	CP-ART-06-2023-003067.R1
Article Type:	Paper
Date Submitted by the Author:	07-Aug-2023
Complete List of Authors:	Gobeze, Habtom; University of Texas at San Antonio, Department of Chemistry Jagadesan, Pradeepkumar; University of Texas at San Antonio, Department of Chemistry Schanze, Kirk; University of Texas at San Antonio, Department of Chemistry

Photophysics and Charge Transfer in Oligo(thiophene) Based Conjugated Diblock Oligomers

Habtom B. Gobeze, Pradeepkumar Jagadesan, and Kirk S Schanze*

University of Texas at San Antonio, Department of Chemistry
One UTSA Circle, San Antonio, TX 78249.
* Corresponding author email: kirk.schanze@utsa.edu

Abstract

This paper reports an investigation of the electronic structure and photophysical properties of two "diblock" π-conjugated oligomers (**T4-TBT** and **T8-TBT**) that feature electron rich tetra(thiophene) (**T_4**) or octa(thiophene) (**T_8**) segments linked to an electron poor 4,7-bis(2-thienyl)-2,1,3-benzothiadiazole (**TBT**) moiety. Electrochemistry and UV-visible absorption spectroscopy reveals that the diblock oligomers display redox and absorption features that can be attributed to the **T_n** and **TBT** units. Density functional theory (DFT) and time-dependent DFT (TDDFT) calculations support the experimental electrochemistry and optical spectroscopy results, suggesting that the frontier orbitals on the diblock oligomers retain characteristics of the individual π-conjugated segments. However, low energy optical transitions are anticipated to arise from **Tn** to **TBT** charge transfer. Fluorescence spectroscopy on the diblock oligomers reveals that the oligomers feature a strongly solvent dependent fluorescence. In non-polar solvents (hexane, toluene), the emission is structured with a moderate Stokes shift; however, in more polar solvents the emission becomes broader, and red-shifts significantly. Transient absorption spectroscopy on timescales from femtoseconds (fs) to microseconds (μs) reveals that in non-polar solvents excitation produces a singlet excited state (LE) that decays uniformly to the ground state in parallel with intersystem crossing to a triplet state. By contrast, in more polar solvents, excitation produces a very short-lived excited state (1 – 3 ps) which evolves rapidly into a second excited state that is attributed to the charge transfer (CT) state. The fast dynamics are associated with crossing from the LE state, which is populated initially by photoexcitation, into the CT state, which then decays to the ground state. The photophysical properties and dynamics of the LE and CT excited states are very similar for **T4-TBT** and **T8-TBT**, suggesting that the length of the oligo(thiophene)

segment does not have a strong influence on the energy, structure or dynamics of the LE and CT excited states.

Introduction

π-Conjugated oligomers and polymers have received considerable attention due to their versatile optical and semiconducting properties as well as for potential applications in electronic, optical, and optoelectronic devices such as transistors, light emitting diodes, photovoltaics, and photodetectors.[1,2] A key advance in the design of π-conjugated oligomers and polymers was the development of donor-acceptor systems that incorporate electron rich and electron deficient moieties into a single π-conjugated segment.[3] The donor-acceptor interactions present in these systems allow tuning of the frontier orbital energy levels and the optical bandgap.[4] These interactions give rise to materials that display improved properties for application, especially in solar cells and photodetectors, where visible and near-infrared light harvesting and exciton splitting into charge carriers are essential to device performance.[5,6]

At a fundamental level, it is important to understand the effects that arise when electron rich (donor) and electron poor (acceptor) units are incorporated into a single π-conjugated segment.[7,8] The frontier orbital energy level offsets present in these systems bear analogy to the band offsets in inorganic semiconductor heterojunctions.[9] The latter are typically characterized as featuring Type I or Type II offsets, corresponding respectively to situations where the bands are nested or offset (Figure 1).[9] We are exploring the electronic structure and excited state behavior of π-conjugated "diblock" oligomers that feature electron rich and electron poor segments that are strongly coupled.[10-12] The goal of this work is to understand the relationship between the excited state properties and electronic structure and interactions between the two conjugated segments. Previous related work in this area includes studies by Yu and co-workers who demonstrated diode

like current rectification in single molecule junctions constructed using oligomers featuring adjacent electron rich and electron poor segments.[13,14]

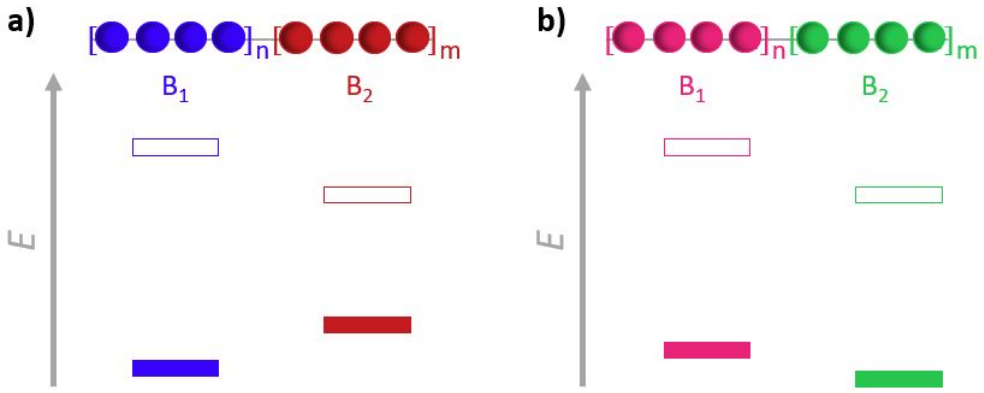

Figure 1. Schematic diagram of electronic band structures of diblock oligomers. Filled rectangles represent filled electron energy levels (e.g. highest occupied molecular orbitals, HOMO) and empty rectangles represent empty electron energy levels (e.g., lowest occupied molecular orbitals, LUMO). a) *Type I* heterojunction where the HOMO/LUMO levels of one block are straddled within the HOMO/LUMO levels of the adjacent block. b) *Type II* heterojunction where there is an energy offset between the levels of adjacent blocks.

The work described herein explores the electronic structure and photophysical properties of two π-conjugated oligomers that feature electron rich oligothiophene (T_n) segments linked to an electron poor 4,7-bis(2-thienyl)-2,1,3-benzothiadiazole (TBT) moiety (Chart 1). In these "diblock" oligomers, the oligothiophene segment serves as an electron donor, and the TBT unit is an acceptor,[7,15] which introduces donor-acceptor interactions between the two conjugated segments. As will be outlined below, these oligomers feature an electronic structure that is analogous to a Type II heterojunction, where the frontier levels of the T_n donor segment are higher and offset compared to the levels on the TBT acceptor. The work has several specific objectives, including 1) delineating the effect of thiophene oligomer on the interaction of locally excited (LE) and charge transfer (CT) excited states; 2) exploring the effect of solvent polarity on the nature of the excited states; 3) examining whether the dynamics of interconversion from locally excited and charge-transfer excited states is influenced by thiophene oligomer length. Although the goal of

this work is to investigate the fundamental aspects of the electronic structure and photophysical properties of the diblock oligomers, these molecules also provide insight into the properties of structurally related donor-acceptor based polymers that have been studied extensively in organic electronic applications. The results described herein build on previous work that has explored donor-acceptor interactions in π-conjugated systems.[16-26]

Chart 1

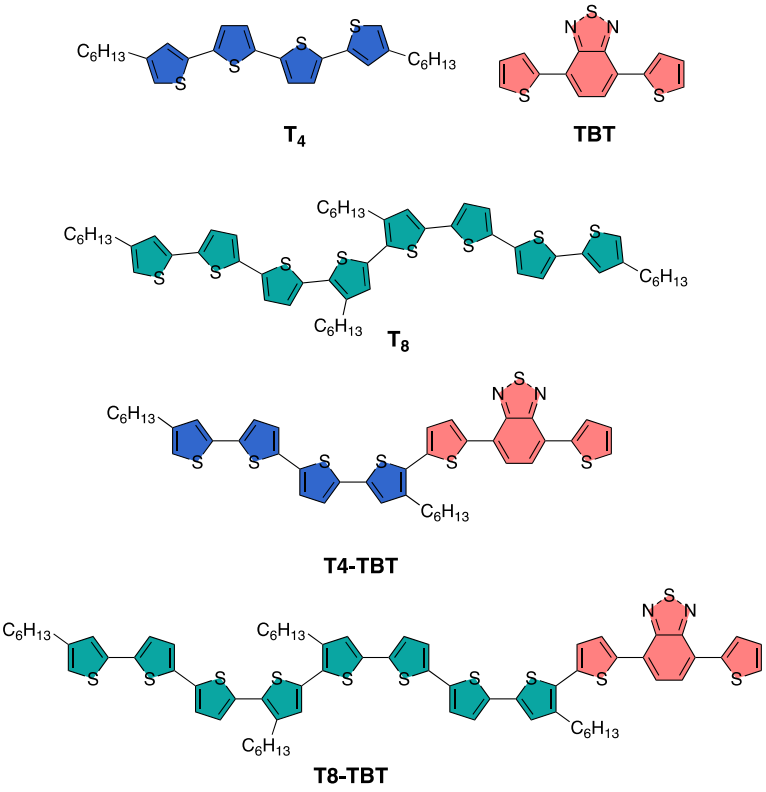

Experimental

Materials. All starting materials and reagents were obtained from commercial sources (Sigma-Aldrich, Fisher Scientific) and used without further purification. Solvents were dried by standard methods or by elution through a MBraun SPS5 solvent purification system. Reactions were performed under a nitrogen atmosphere unless stated otherwise. Thin-layer chromatography (TLC) was conducted with TLC silica gel plastic plates and visualized with UVGL-15 compact

lamps (254/365 nm). Flash chromatography was performed using a Teledyne automated flash chromatography system using RediSep Rf normal-phase silica flash columns (60 Å; particle size 35-70 μm, 230 x 400 mesh). Detailed synthetic schemes, description of methods and spectroscopic characterization data are provided in the supporting information section.

Characterization Methods. ^{1}H and ^{13}C NMR spectra were recorded in $CDCl_3$ using a 500 MHz spectrometer (with TMS as an internal standard). Chemical shifts are reported in parts per million (ppm, δ) using the solvent as the internal standard. The coupling constants are reported in Hertz (Hz). Splitting patterns are designated as s (singlet), bs (broad singlet), d (doublet), t (triplet), and m (multiplet). UV-visible absorption spectra were recorded using a Shimadzu UV-2600 spectrophotometer. Steady-state fluorescence spectra were obtained with an Edinburgh FLS1000 fluorometer. The fluorescence spectra are corrected for the instrument spectral response (detector and monochromator wavelength response) using correction factors provided by the manufacturer. Square Pyrex (1 cm^2) cuvettes were used for solution spectra, and emission was collected at 90° relative to the excitation beam. Absolute fluorescence quantum yields were obtained using an integrating sphere. The optical density of solutions at the excitation wavelength was ≤ 0.1. Fluorescence lifetimes were measured in a PicoQuant FluoTime 300 fluorescence lifetime spectrophotometer by time-correlated single photon counting (PicoQuant PicoHarp 300 module). An LDH-D-C-405 PicoQuant diode laser provided the excitation at 405 nm (repetition rate 40 MHz, power < 3mW) for all samples. The instrument response function (ca. 100 ps fwhm) was measured using a Ludox scattering solution. Decays were obtained using the single/biexponential fitting parameters using FluoroFit software.

Nanosecond transient absorption measurements were acquired with optical parametric oscillator excitation at 410 nm (8-10 mJ/pulse) Opotek Radiant 355 LD series laser. A xenon lamp

in an Edinburgh LP980 spectrometer was used as a probe source. The transient absorption signal was detected with a gated-intensified CCD camera, while the kinetic traces were measured with a PMT and a digital oscilloscope. Samples were prepared to an optical density of 0.5 at the excitation wavelength in a 1 cm path length Pyrex cuvette. Triplet lifetimes were acquired with a single exponential fitting of the transient absorption decay data using Edinburgh L900 software.

Femtosecond-picosecond transient absorption spectroscopy was carried out using a system consisting of a Coherent Astrella Ti:sapphire (100 fs, 1 kHz repetition) source[27] coupled with an Opera Solo OPA[28] and a Ultrafast Systems Helios transient absorption spectrometer.[29] The first beam generated from Coherent Astrella was directed through the optical parametric amplifier, where the wavelength was tuned to 380 – 520 nm. The excitation beam was then directed into a Helios fire (Ultrafast) automated femtosecond transient absorption spectrometer where it was passed through a chopper, depolarizer and neutral density filter to tune the power to 0.1 mW (100 nJ/pulse) prior to incidence on the stirred sample (O.D. ≈ 0.2). The second beam was passed through a digitally controlled delay stage with a maximum range of 8 ns, afterward the beam was focused into a sapphire crystal to generate visible probe ranging from 420 - 700 nm. The NIR probe was generated using a proprietary crystal (Ultrafast Systems) producing a light source spanning from 820 - 1600 nm. The two beams overlap at the sample position with their respective electronic polarizations at the magic angle. The output signal with and without pumping (at several time delays) was detected using a fiber-coupled alignment-free spectrometer with a 1024-pixel CMOS sensor. Chirp, time-zero, and solvent response corrections were employed using the software supplied by Ultrafast Systems where global analysis was done by reconstructing the spectra from two principal component eigenspectra with their associated lifetimes. OriginLab

Corporation (version 9.55) data analysis software was used to plot the spectra. Glotaran software was used to carry out global analysis of the time-resolved spectroscopic data.[30]

Results

Structures and Synthesis. The synthesis of the compounds investigated including thiophene oligomers **T4** and **T8** and diblock oligomers **T4-TBT** and **T8-TBT** is outlined in the supporting information section. The compounds were characterized by ^{1}H and ^{13}C NMR and high-resolution mass spectroscopy. The thiophene oligomers feature hexyl solubilizing chains, and the TBT moiety is attached to the oligothiophene segment by a direct link to the terminal thiophene unit of a T_4 or T_8 oligomer.

Electrochemistry and DFT Calculations. Electrochemistry and density functional theory calculations (DFT) were carried out to probe the electronic structure and frontier energy levels of the oligomers. Electrochemistry was studied in N_2 saturated dichloromethane solutions using a standard three electrode cell by cyclic voltammetry and potentials are referenced to an Fc^{+}/Fc internal standard. The first oxidation and reduction potentials ($E^{ox}_{1/2}$ and $E^{red}_{1/2}$, respectively) are listed in Table 1, and the cyclic voltammograms are shown in Figure S5. Consistent with previous

Table 1. Electrochemical Potentials

	$E_{1/2}/V$			
Compound	**red**	**Ox_1**	**Ox_2**	**$\Delta Eg/eV$**
T4	-	0.49	0.75	-
T8	-	0.25	-	-
TBT	-1.60	0.87	-	-
T4-TBT	-1.69	0.55	1.59	2.24[b]
T8-TBT	-1.66	0.26	-	1.92[b]

[a] In nitrogen saturated dichloromethane with 0.1 M tetrabutyl ammonium hexafluoro phosphate as a supporting electrolyte in a three-electrode set up with glassy carbon (WE), silver/silver chloride (RE), and platinum wire (CE) and a scan rate of 100 mVs^{-1}. The redox values are referenced vs Fc/Fc^{+} potential. [b] Obtained from the difference of $E_{1/2ox1}$ and $E_{1/2red}$.

reports, the thiophene oligomers, **T4** and **T8**, reveal reversible first oxidation peaks with $E^{ox}_{1/2}$ values of 0.49 V and 0.25 V, respectively.[31] As the number of thienylene repeating units increases from **T4** to **T8**, the first oxidation potential decreased by ~250 mV. In the accessible cathodic potential range (to -1.7 vs Fc^+/Fc), neither **T4** or **T8** reveals a reduction wave, consistent with comparatively high LUMO energy levels. A similar observation was also reported before in a series of thiophene oligomers and their naphthalimide acceptor derivatized counterparts.[31] On the other hand, the **TBT** model compound reveals a well-resolved, reversible reduction potential with $E^{red}_{1/2}$ = -1.66 V.

The diblock oligomers **T4-TBT** and **T8-TBT** exhibit electrochemical waves that appear as a sum of the individual components. In particular, **T4-TBT** and **T8-TBT** feature first oxidations at 0.55 and 0.26 V which are very close to the potentials of the corresponding model thiophene oligomers. Moreover, both diblock oligomers reveal a single reversible reduction wave, at potentials very close to the reduction potential of the **TBT** model. These observations indicate that the covalent link between the T_n and TBT units has only a small effect on the energies of the T_n localized occupied levels (HOMO) and the TBT localized unoccupied levels (LUMO).

To visualize the spatial distribution of the frontier orbitals and to calculate the energy levels, calculations using DFT at a theory level of B3LYP and a basis set of 6-31/G (d, p) were performed. The combination of the theory and the basis set was used because they were previously shown to predict with reasonable accuracy the frontier orbitals and energies of π-conjugated thiophene oligomers.[32,33] Plots of the electron density for the HOMOs and LUMOs for the di-block oligomers are shown in Figs. 2b and d, and the calculated orbital energies are displayed in the diagram in Figs 2a and c, while the frontier orbitals for the model compounds are shown in Figure S6 and their energies are included in Figs. 2a and c and in Table S1. The DFT calculated energies

corroborate the electrochemically obtained redox potentials. Consistent with the trend in the measured potentials, the HOMO of **T8** is at higher energy than that of **T4**. In addition, the calculated LUMO energies reveal that **TBT** has a much lower LUMO energy compared to **T4** and **T8**. Interestingly, the density plots (Figs. 2b and d) reveal that for both **T4-TBT** and **T8-TBT**, the HOMO is largely delocalized across the entire oligomers; however, the LUMO is mainly concentrated in the TBT moiety.

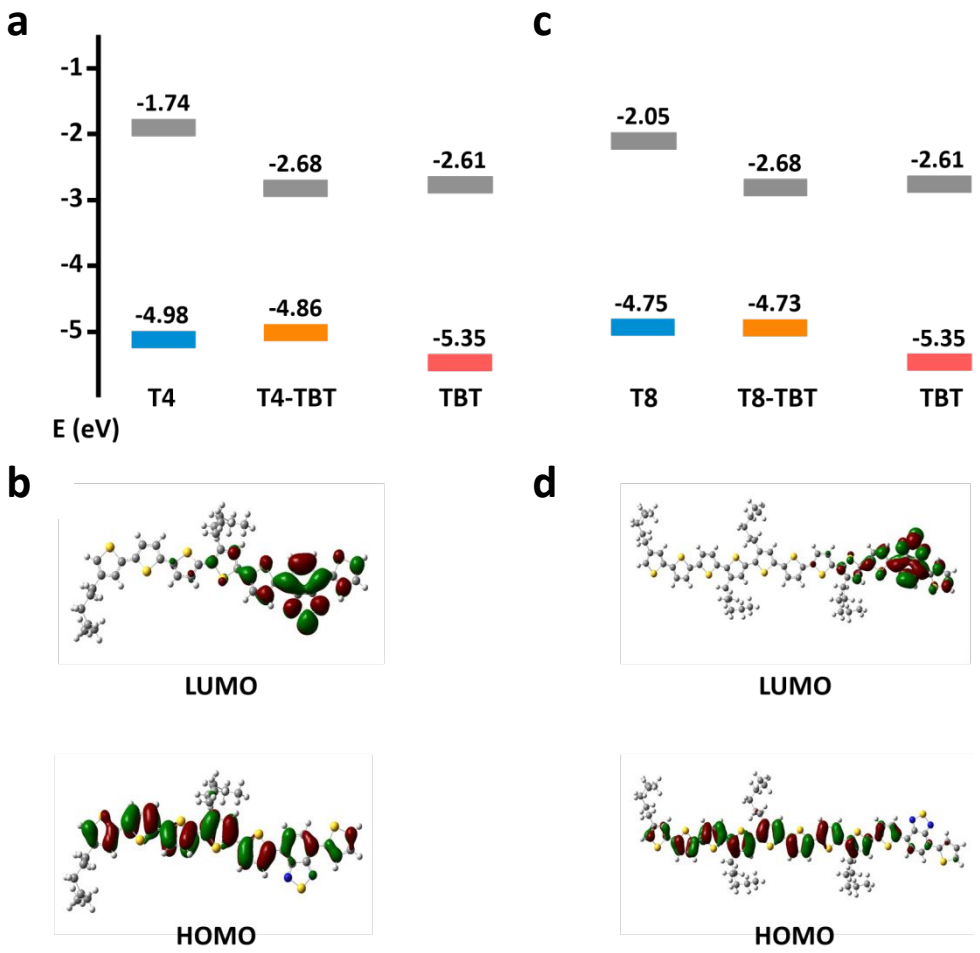

Figure 2. HOMO and LUMO energy levels of **T4**, **T4-TBT**, and **TBT** (a), and of **T8**, **T8-TBT**, and **TBT** (c). Orbital electron density plots for HOMO and LUMO levels of **T4-TBT** (b) and of **T8-TBT** (d).

Photophysical Characterization. UV-visible absorption spectra of the **Tn-TBT** di-block oligomers and the model compounds were studied in several solvents of differing polarity. Figs. 3a and c show the normalized absorption spectra of **T4-TBT** and **T8-TBT**. The spectra plotted

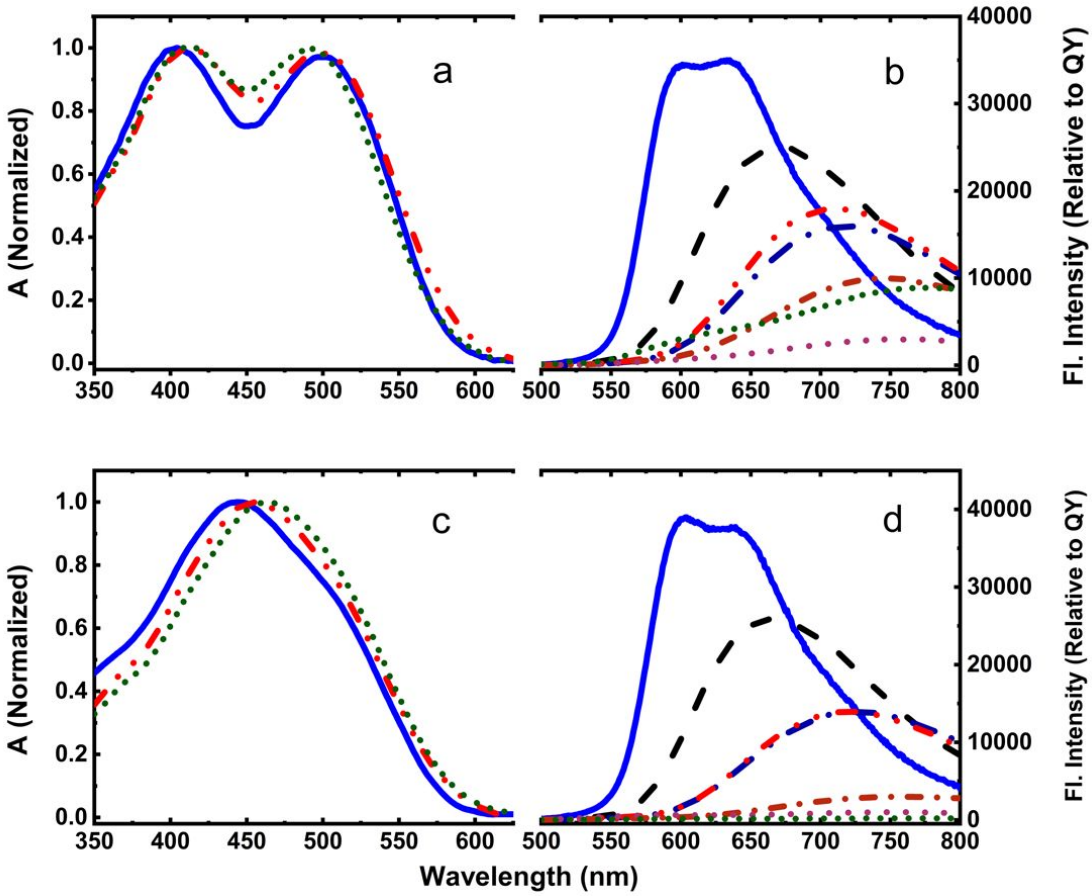

Figure 3. Absorption spectra of **T4-TBT** (a) and **T8-TBT** (c) in hexane (solid line, blue), tetrahydrofuran (dash dot dot, red), and dimethylformamide (dotted, green). Fluorescence emission spectra of **T4-TBT** (b) and **T8-TBT** (d) in hexane (solid line, blue), diethyl ether (dashed line, black), chloroform (dash dot, dark blue), tetrahydrofuran (dash dot dot, red), dichloromethane (dash dot, dark red), acetone (dotted, purple), dimethylformamide (doted, green). The relative intensity of the fluorescence spectra reflect the relative quantum yields in the different solvents (see Table 2).

vs. molar absorption coefficient **T4-TBT** and **T8-TBT** and the corresponding model compounds (**T4**, **T8** and **TBT**) are shown in Fig. S11. **T4-TBT** features two distinct absorption bands; the long wavelength band is associated with a π,π* transition with charge-transfer (CT) character, whereas the shorter wavelength band is a π,π* transition which is contributed mainly by the T4 segment. These spectral assignments are supported by time-dependent DFT calculations (TDDFT)

which show that the orbital basis for the long-wavelength transition is dominated by the HOMO-LUMO excitation which displaces charge from the T4 segment to the TBT acceptor (Figs. S7 and S8). By contrast, TDDFT indicates that the higher energy band is associated with excitations mainly localized on T4.

The absorption of **T8-TBT** presents as a single, broad band. It is likely that this band has contributions on the long-wavelength side due to a π,π^*/CT transition whereas the main intensity near the maximum is contributed by a π,π^* transition that is mainly localized on the T8 segment. (These assignments are supported by the comparison of spectra shown in Fig. S11 and the TDDFT results in Figs. S9 and S10). The absorption spectra of **T4-TBT** and **T8-TBT** exhibit a weak solvent dependence, with the latter showing a small, but noticeable red-shift with increasing solvent polarity. This effect is consistent with an excited state having a greater dipole moment compared to the ground state.

The fluorescence spectra of **T4-TBT** and **T8-TBT**, shown in Figs. 3b and d, are strongly solvent dependent. In the lowest polarity solvent (hexane), the emission of both oligomers exhibits weak vibronic coupling, with several peaks resolved. However, with increasing solvent polarity the fluorescence spectra broaden and red-shift with increasing solvent polarity. (By comparison, the model oligomers **T4** and **T8** exhibit little solvatochromism in the emission, Figs. S12 and S13). Notably, the fluorescence maxima of **T4-TBT** and **T8-TBT** are similar in most of the solvents studied. In addition to the red-shift in the emission, the quantum yields and lifetimes also decrease with increasing solvent polarity (Table 2). While the solvent induced variation of the fluorescence is profound for both **T4-TBT** and **T8-TBT**, the effect is even larger for the latter, where the emission quantum yield varies from 0.39 in hexane to 0.002 in DMF solution. Radiative and non-radiative decay rates (k_r and k_{nr}, respectively) were calculated from the fluorescence parameters

(Table S4). It is seen that for both oligomers in hexane k_r and k_{nr} are typical for π-conjugated oligomers (e.g., ~ 10^8 s^{-1}).[34] However, for both oligomers in solvents of increasing polarity, k_r decreases and k_{nr} increases, with both rates varying by more than an order of magnitude over the solvents studied.

Table 2. Fluorescence Quantum Yields and Lifetimes[a]

	T4-TBT				T8-TBT				
Solvent	**λ_{em} / nm**	**Φ_{fl} [b]**	**τ_1 / ns [c]**	**τ_2 / ns [c]**	**λ_{em} / nm**	**Φ_{fl} [b]**	**τ_1 / ns [c]**	**τ_2 / ns [c]**	**τ_3 / ns [c]**
Hex	600	0.35	1.8	-	604	0.39	1.5	-	-
Et_2O	669	0.25	1.6	-	665	0.26	1.5	-	-
THF	714	0.18	1.4 (0.98)	13 (0.02)	719	0.14	1.1	-	-
$CHCl_3$	714	0.16	1.3	-	724	0.14	1.1	-	-
DCM	741	0.10	1.3	-	760	0.03	0.4 (0.85)	1.4 (0.15)	
Ace	756	0.03	0.4 (0.97)	1.0 (0.03)	761	0.01	0.1 (0.67)	0.8 (0.26)	3.57 (0.07)
DMF	782	0.09	0.2 (0.99)	3.4 (0.01)	760	0.002	0.06 (0.9)	0.8 (0.07)	4.0 (0.03)

[a] Solvents: Hex = hexane, Et_2O = diethylether, THF = tetrahydrofuran, $CHCl_3$ = chloroform, DCM = dichloromethane, Ace = acetone, and DMF = dimethylformamide. [b] Absolute fluorescence quantum yields were determined using integrating sphere. [c] Fluorescence lifetimes were measured using the TCSPC method. For all the samples, an excitation wavelength of 405 nm was used, and the decays were monitored at the maximum fluorescence wavelength. Where more than one component is listed, numbers in parentheses indicate the relative amplitude of the decay component.

Taken together the fluorescence results are consistent with the emission arising from an excited state having substantial charge-transfer character, with the degree of charge-transfer increasing with solvent polarity.[35] To estimate the change in dipole moment between the ground and excited state with respect to the Stokes shift as solvent polarity increases, the Lippert-Mataga analysis[36] was used and the obtained change in dipole moments are 17 (± 5) and 22 (± 5) Debye for **T4TBT** and **T8TBT**, respectively. (See Figure S15 and the associated text and equations. Note that the difference dipole moments for the two oligomers are not distinguishable within experimental uncertainty.)

Transient Absorption Spectroscopy. Transient absorption (TA) spectroscopy was performed on the oligomers on timescales ranging from sub-ps to μs using femtosecond and nanosecond pump-probe spectroscopy. The time resolved TA difference spectra for **T4-TBT** and **T8-TBT** in non-polar and moderately polar solvents on timescale from 1 ps – 7 ns are shown in Figs. 4 and 5 and spectra obtained at longer delay times (10 ns – 10 μs) are shown in the Figs. S17 and S18 in the supporting information. A previous study reported the TA spectra and dynamics for **T4** and **T8** on ps - μs timescales.[37,38]

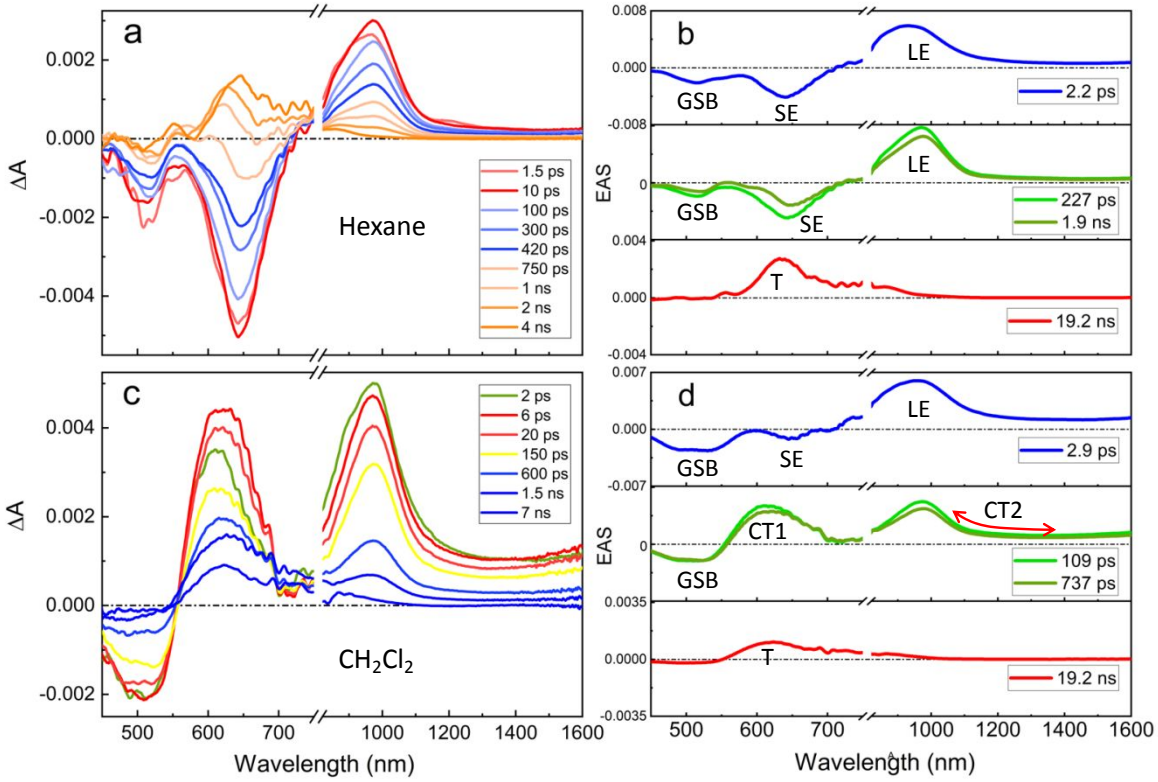

Figure 4. Femtosecond transient absorption and evolution associated spectra obtained from global analysis for **T4-TBT** in hexane (a and b) and in dichloromethane (c and d), respectively.

The TA spectra and dynamics of **T4-TBT** and **T8-TBT** in non-polar solvents (hexane and toluene, respectively) are similar (Figs. 4a and 5a). At early delay times, the spectra in the visible region are dominated by negative TA bands, corresponding to bleach of the ground state absorption (GSB, ~500 nm, GSB) and stimulated emission (SE, ~650 nm). In both **T4-TBT** and **T8-TBT** the

SE red shifts at early delay times, 1-20 ps. This was previously observed in the picosecond timescale TA spectra of **T4** and **T8** and was attributed to conformational relaxation within the T_n segments.[38] In the near-IR both oligomers display strong and broad excited state absorption (ESA) with peak ~1000 nm. Note that the near-IR absorption of **T8-TBT** is substantially broader on the long-wavelength side, with significant amplitude beyond 1600 nm. These features decay on the 100 – 1000 ps timescale, evolving into spectra with broad absorption in the 600 – 650 nm region that does not decay within 5 ns. These long-time spectra are like those observed by ns - μs TA (Fig. S17 and S18) and thus are attributed to the oligomers' triplet excited states.

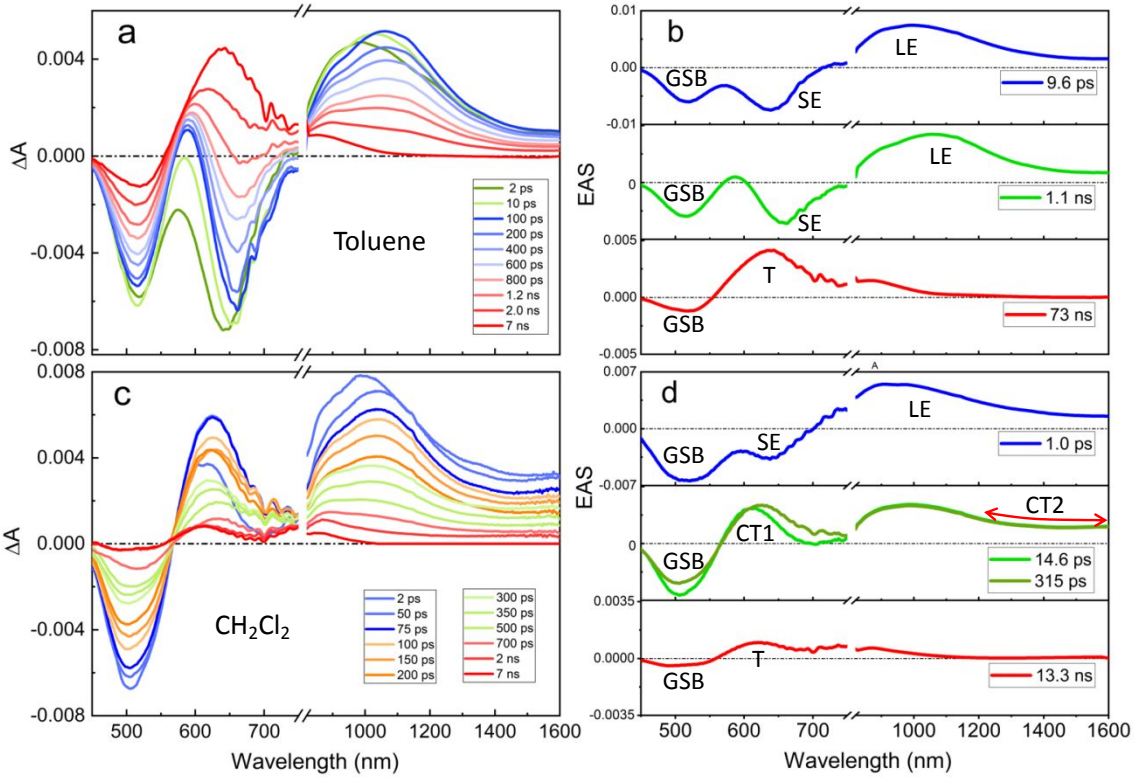

Figure 5. Femtosecond transient absorption and evolution associated spectra obtained from global analysis for **T8-TBT** in toluene (a and b) and in dichloromethane (c and d), respectively.

The ps spectra of **T4-TBT** and **T8-TBT** in more polar solution (CH_2Cl_2) are distinctly different from those seen in the less polar media (Figs. 4c and 5c). The most obvious difference is the absence of the SE and the instantaneous appearance of positive bands due to ESA at ~600

nm in the visible region and a broad near IR signal in the wavelength range of 1200 -1600 nm. Interestingly, in the more polar CH_2Cl_2 environment, the near-IR ESA is even broader and more intense on the long wavelength side of the main absorption peak (λ > 1200 nm). This feature has been observed in previous studies of acceptor substituted oligothiophenes, and it has been attributed to the polaron (cation radical) absorption of the oligomer in a charge-transfer excited state. [31,37-41] At long delay times (> 5 ns), the visible and near-IR ESA features decay, leaving a weak transient absorption feature at ~630 nm that is attributed to the triplet excited state. Note that for both **T4-TBT** and **T8-TBT** the residual triplet absorption is weaker in CH_2Cl_2 compared to the less polar solvents, suggesting that the triplet yield is suppressed in the more polar solvent.

To determine the principal spectral components and their corresponding decay lifetimes, the ps TA data of **T4-TBT** and **T8-TBT** was analyzed by using global kinetic analysis.[30] All data in both polar and nonpolar solvents are well-fitted to three (or four)[42] components and the un-normalized evolution associated spectra (EAS) along with the decay lifetimes associated with each spectral component are shown in Figs. 4b,d and 5b,d (right panels). Note that the amplitude of each EAS reflects the relative contribution of the spectral-kinetic component to the total transient absorption spectrum (e.g., a low amplitude on the EAS reflects a minor contribution to the total spectrum). Comparison of the EAS for **T4-TBT** and **T8-TBT** reveal important features. First, in the non-polar solvents studied (hexane and toluene), the global analysis reveals three kinetic components (fast, middle, slow). For both **T4-TBT** and **T8-TBT** the fast and middle EAS components are similar, with two negative features in the visible (GSB and SE) and one absorption feature (LE). The GSB feature is attributed to ground state absorption bleach, SE to stimulated emission, and LE is excited state absorption. The slow EAS component exhibits a single absorption feature (T), which is clearly due to the triplet state. The results in the non-polar solvent

suggest that the initially produced excited state persists until it decays leaving the triplet state. The fast relaxation process (fast -> middle) is likely due to inner- and outer-sphere relaxation of the initially produced excited state.

In the more polar CH_2Cl_2 solvent, for both **T4-TBT** and **T8-TBT** the fast and middle EAS components are distinctly different. The fast component in CH_2Cl_2 is very similar in appearance to the fast and middle components seen in the non-polar solvents; however, the middle EAS component is different, with one ground state bleach (GSB) and two absorption features, one in the visible (CT1) and the second a very broad feature with a tail in the near-IR (CT2). These results suggest that in the polar solvent, initial excitation produces an excited state that evolves rapidly (1 – 3 ps) into a second excited state. As discussed below, we hypothesize that the initial excited state is a locally excited state (LE) and this evolves within several ps into a T_n to TBT charge transfer (CT) state. Note that for both **T4-TBT** and **T8-TBT** in CH_2Cl_2 the slow EAS component associated with the triplet state (T), has a much smaller amplitude compared to the non-polar solvent; this implies that the triplet yield is suppressed in the polar solvent.

Discussion

A primary objective of the current study was to characterize the structure and dynamics of the excited states in the set of diblock oligomers that feature T_n and TBT segments and how they vary with solvent polarity and oligo(thiophene) length. As noted above, the T_n and TBT segments feature distinct frontier orbital energy levels and bandgaps. At the outset, we anticipated that two primary processes that may occur in the excited state would be 1) energy transfer from T_n to the TBT segment, or 2) formation of a T_n to TBT charge transfer excited state. Also of interest was involvement of oligo(thiophene) localized excited states that are produced at early times following photoexcitation, and if these are observed, what are the dynamics for excited state evolution. The

electrochemical and DFT calculations both point to the possibility that charge transfer will dominate the excited states of the diblock oligomers, and as discussed below, this is borne out by the results of the emission and transient absorption experiments.

As seen in Fig. 3, the fluorescence of both **T4-TBT** and **T8-TBT** is strongly solvatochromic: the fluorescence of both undergoes a significant shift to longer wavelength (lower energy) with increasing solvent polarity. Coupled with the red shift, the fluorescence quantum yields and lifetimes also decrease with increasing solvent polarity. These fluorescence properties are hallmarks of chromophores that emit from an excited state with charge transfer character.[43-46] The fluorescence in non-polar solvents is similar in band shape to that of the parent oligo(thiophene)s (**T4** and **T8**, Figs. S12 and S13); however, it is red shifted significantly in the diblock oligomers from the position in the respective oligo(thiophene). The emission in non-polar solvents from the diblocks is also distinct from the **TBT** model (Fig. S14), which emits a single broad band at shorter wavelength. Taken together, these results imply that in non-polar solvents, the excited state in **T4-TBT** and **T8-TBT** is fully delocalized, but it does not have a substantial degree of CT character. We refer to this delocalized, non-CT state as the LE state. (The notation "LE" in the TA in Figs. 4 and 5 refers to this non-CT state, which is also represented by the black potential energy curve in Scheme 1.) By contrast, as solvent polarity increases, the degree of CT character in the excited state increases and becomes substantial in the more polar environments.

Interestingly, the emission spectra for **T4-TBT** and **T8-TBT** have very similar λ_{max} values in the solvents studied, and the Lippert-Mataga plots for the two oligomers are parallel (Fig. S15). These findings suggest that the energy and difference dipole moments of the CT excited state are nearly the same for the two oligomers. This is an important finding, as it suggests that the structure and energy of the of the relaxed CT state is not strongly influenced by the difference in length of

the oligo(thiophene) segments. Figure 6 show plots of the emission energy of **T4-TBT** and **T8-TBT** as a function of the solvent dielectric. This figure highlights the fact that the emission energy of the two oligomers is nearly the same, regardless of solvent polarity. In the same figure we also compare the calculated energies of the CT state for the two oligomers according to the equation provided in the SI section (eq. S1).[47-49] This calculation assumes that unit charge transfer occurs between the oligo(thiophene) and the TBT acceptor, and that the charge separation distance is taken as the distance from the center of the oligo(thiophene) segment to the TBT unit. Note that the calculated energy of the CT state for the two oligomers differs by ~300 meV in all the solvents examined; this difference mainly reflects the difference in the oxidation potential of the oligo(thiophene) units (see Table 1).

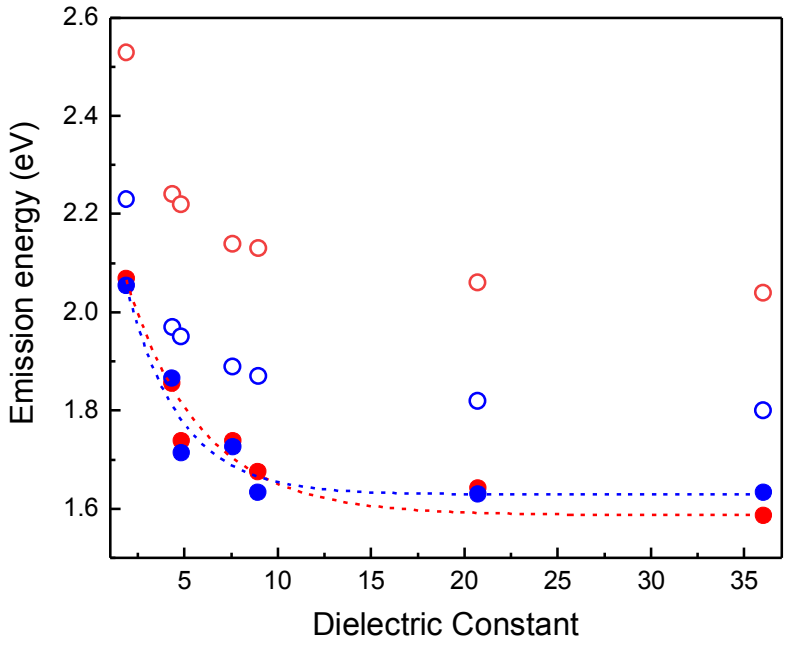

Figure 6. Plots of experimental and calculated emission energies for **T4-TBT** (red) and **T8-TBT** (blue). Experimental data points are filled circles (●)and calculated data are unfilled circles (○). Dashed lines through experimental data are drawn to guide the eye. Calculated energies using eq. S1 in supporting information section.

There are two key conclusions that can be drawn by comparison of the plots in Fig. 6. First, the energy of the CT state that is experimentally observed is lower than the calculations estimate

for both oligomers. We attribute this difference as arising because the degree of charge transfer in the CT state is less than complete unit electron transfer (eq. S1 which is used to compute the CT state energy assumes unit electron transfer from donor to acceptor). There may also be contributions to lowering the CT state energy that arise due to delocalization of the positive charge in the oligo(thiophene) unit that is not well modeled by the theory.[49] Secondly, and perhaps more important, is the fact that the energy of the CT state is almost the same in the two oligomers. This feature strongly suggests that in **T4-TBT** and **T8-TBT** the CT excitation is more strongly localized on the TBT moiety with some delocalization of positive charge into the oligo(thiophene) segment. However, given the similar energy of the CT state, the delocalization of the positive charge in the oligo(thiophene) segment is similar in **T4-TBT** and **T8-TBT**.

With the hypothesis that there are two predominant states for the diblock oligomers, namely LE and CT, we turn to apply this concept to an analysis of the transient absorption spectra and dynamics. First, in non-polar solutions, the shape of the visible-near-IR TA spectra for both diblock oligomers are relatively invariant over the time-scale of 100 fs – 1 ns, suggesting that the state that is initially produced by photoexcitation persists into the ns time domain, ultimately decaying to form a longer-lived triplet state. This excited state is characterized by three features that are resolved in the evolution associated spectra (EAS, right panels in Figs. 4 and 5) due to ground-state bleaching (GSB), stimulated emission due to fluorescence (SE), and an absorption band in the near-IR that is due to the locally-excited singlet state (LE). The LE band in the near-IR is red-shifted and broader in **T8-TBT** compared to **T4-TBT**. The initially excited state undergoes an ultrafast relaxation (~2 ps in **T4-TBT** and ~10 ps in **T8-TBT**) that is likely associated with conformational relaxations in the excited state oligomers.[37,38] The remainder of the decay of

the LE state occurs on the ns timescale, with lifetimes that are in good agreement with the fluorescence lifetimes in non-polar solvent (Table 2).

In the more polar solvent studied (dichloromethane, DCM), there are distinct changes in the visible-near-IR TA spectra that occur on the ultrafast timescale. This is most evident from inspection of the EAS in Figs. 4 and 5. Here it is seen that the first EAS component for both diblock oligomers is similar to the spectra in non-polar solvents. Specifically, the EAS component exhibits negative features in the visible region due to GSB and SE, and a near-IR band labeled LE. This first component decays very rapidly (~3 ps for **T4-TBT** and ~1 ps for **T8-TBT**), evolving into a second component that is distinct, with two prominent absorption bands, one near 650 nm in the visible and the second is a broad band that tails well into the near-IR (CT1 and CT2, respectively). Both absorption features are clearly associated with (partial) positive charge on the thiophene segment that exists in $T_n \rightarrow$ TBT charge transfer excited state. Similar absorption features were observed for the CT state in a recent study of oligo(thiophene)s capped with a strong naphthalene diimide electron acceptor.[31] The ultrafast dynamics that are seen for **T4-TBT** and **T8-TBT** in DCM are attributed to relaxation from the LE state that is initially populated by photoexcitation, into the CT state.

Scheme 1 provides an excited state scheme for the diblock oligomers that is based on the hypothesis that there are two predominant excited states, namely LE in which the excitation is mainly localized on the TBT moiety with declocalization into the oligo(thiophene) segment, and a CT in with there is partial charge transfer from the oligo(thiophene) segment acting as a donor to the TBT unit as the acceptor. Excitation of the diblocks in all solvents initially accesses the LE state. In non-polar solvents, the CT manifold is higher in energy and therefore it is not populated. The LE state decays by radiative and non-radiative channels, and undergoes intersystem crossing

to afford a triplet excited state. By contrast as the solvent becomes more polar, the energy of the CT state decreases relative to the LE and crossing from LE to CT becomes the dominant process that occurs with a rate greater than 10^{11} s^{-1}. Since the CT state is lower in energy, intersystem crossing becomes less efficient, and it does not occur to any extent in very polar solvents.

Scheme 1

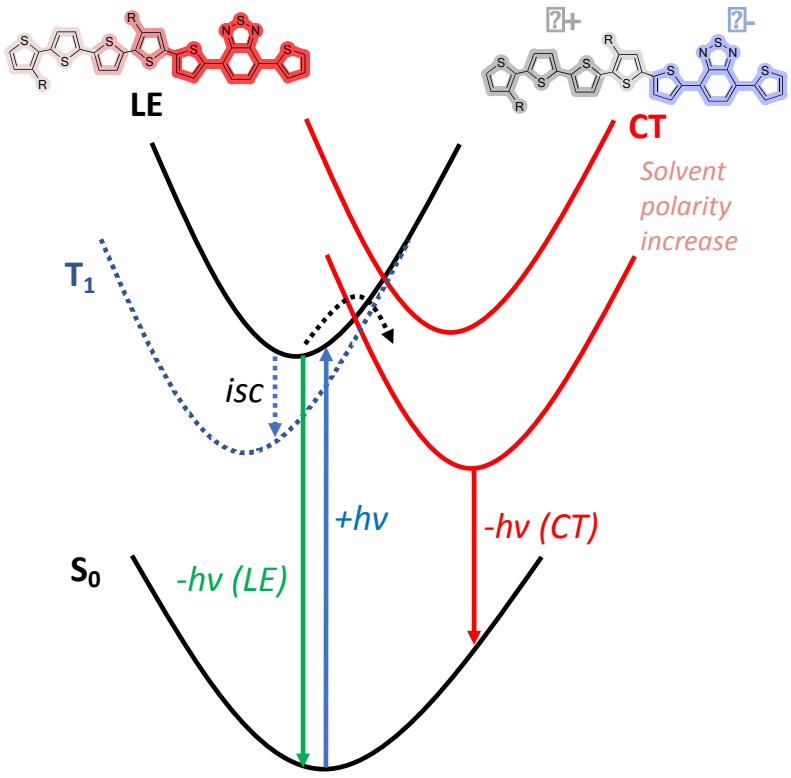

Conclusion

A detailed photophysical study has been carried out on two diblock π-conjugated oligomers that feature oligo(thiophene) segments linked to TBT. The absorption spectra and electrochemical results reveal signatures of each of the conjugated segments. In particular, absorption features can be attributed to the oligo(thiophene) and TBT segments, and the first oxidation and reduction processes are associated with the individual units. Analysis of the fluorescence results reveals that the emission of the diblock oligomers is strongly solvent dependent, which suggests that in polar

solvents the lowest energy state has charge transfer character. Femtosecond-picosecond time resolved absorption spectroscopy shows that the excited state absorption of the diblock oligomers is distinct in non-polar and polar solvents. This behavior is attributed to the hypothesis that in non-polar solvents, the singlet excited state is a delocalized state without significant charge transfer character, but in more polar solvents the excited state has charge transfer character.

An important question concerns how the work that is reported in this paper translates to properties of diblock oligomers and structurally related polymers in the solid state which is relevant to their use in organic electronic devices.[7] We suspect that given the predominance of charge transfer in the excited states of these diblock oligomers in solution, that this will translate to the solid state, where intramolecular and intermolecular charge transfer could take place. This will be the focus future work from these laboratories using **T_n-TBT** and structurally related diblock oligomers and polymers.

Acknowledgements

This work is supported by the Air Force Office of Scientific Research under Grant No. W911NF-20-1-0301 (AFOSR Materials Chemistry Program, Dr. Kenneth Caster Program Officer). Partial support is provided by the Welch Foundation through the Welch Chair at the University of Texas at San Antonio (Award No. AX-0045-20110629).

References

1. *Handbook of Conducting Polymers, 4th Edition*, CRC Press, Boca Raton, 2019.
2. K. Müllen and G. Wegner, *Electronic Materials: The Oligomer Approach*, Wiley-VCH, Weinheim, 2008.
3. Y.-J. Cheng, S.-H. Yang and C.-S. Hsu, *Chem. Rev.*, 2009, **109**, 5868-5923.
4. P. M. Beaujuge, C. M. Amb and J. R. Reynolds, *Acc. Chem. Res.*, 2010, **43**, 1396-1407.
5. T. Xu and L. Yu, *Materials Today*, 2014, **17**, 11-15.
6. D. Zhu, D. Ji, L. Li and W. Hu, *J. Mater. Chem. C*, 2022, **10**, 13312-13323.

7. M. Scarongella, A. Laktionov, U. Rothlisberger and N. Banerji, *J. Mater. Chem. C*, 2013, **1**, 2308-2319.
8. I. Hwang, S. Beaupré, M. Leclerc and G. D. Scholes, *Chemical Science*, 2012, **3**, 2270-2277.
9. S. A. Ivanov, A. Piryatinski, J. Nanda, S. Tretiak, K. R. Zavadil, W. O. Wallace, D. Werder and V. I. Klimov, *J. Am. Chem. Soc.*, 2007, **129**, 11708-11719.
10. A. L. Jones, J. Jiang and K. S. Schanze, *J. Am. Chem. Soc.*, 2020, **142**, 12658-12668.
11. M. Younus, S. Valandro, H. B. Gobeze, S. Ahmed and K. S. Schanze, *J. Photochem. Photobiol. A*, 2023, **435**, 114303.
12. H. B. Gobeze, D. Martinez and K. S. Schanze, *J. Photochem. Photobiol. A*, 2023, **444**, 114966.
13. M.-K. Ng, D.-C. Lee and L. Yu, *J. Am. Chem. Soc.*, 2002, **124**, 11862-11863.
14. W.-Y. Lo, N. Zhang, Z. Cai, L. Li and L. Yu, *Acc. Chem. Res.*, 2016, **49**, 1852-1863.
15. P. M. Beaujuge, C. M. Amb and J. R. Reynolds, *Acc. Chem. Res.*, 2010, **43**, 1396-1407.
16. J.-L. Brédas, D. Beljonne, V. Coropceanu and J. Cornil, *Chem. Rev.*, 2004, **104**, 4971-5004.
17. J. Huang, Y. Wu, H. Fu, X. Zhan, J. Yao, S. Barlow and S. R. Marder, *J. Phys. Chem. A*, 2009, **113**, 5039-5046.
18. I. Botiz, R. D. Schaller, R. Verduzco and S. B. Darling, *J. Phys. Chem. C*, 2011, **115**, 9260-9266.
19. S. R. González, J. Orduna, R. Alicante, B. Villacampa, K. A. McGee, J. Pina, J. Seixas de Melo, K. M. Schwaderer, J. C. Johnson and B. A. Blackorbay, *J. Phys. Chem. B*, 2011, **115**, 10573-10585.
20. K. Johnson, Y.-S. Huang, S. Huettner, M. Sommer, M. Brinkmann, R. Mulherin, D. Niedzialek, D. Beljonne, J. Clark and W. T. Huck, *J. Am. Chem. Soc.*, 2013, **135**, 5074-5083.
21. E. N. Hooley, D. J. Jones, N. C. Greenham, K. P. Ghiggino and T. D. Bell, *J. Phys. Chem. B*, 2015, **119**, 7266-7274.
22. L. Zaikowski, G. Mauro, M. Bird, B. Karten, S. Asaoka, Q. Wu, A. R. Cook and J. R. Miller, *J. Phys. Chem. B*, 2015, **119**, 7231-7241.
23. J. Jiang, A. Alsam, S. Wang, S. M. Aly, Z. Pan, O. F. Mohammed and K. S. Schanze, *J. Phys. Chem. A*, 2017, **121**, 4891-4901.
24. V. Maffeis, R. Brisse, V. Labet, B. Jousselme and T. Gustavsson, *J. Phys. Chem. A*, 2018, **122**, 5533-5544.

25. J. T. Buck, R. W. Wilson and T. Mani, *J. Phys. Chem. Lett.*, 2019, **10**, 3080-3086.
26. X. Niu, P. Gautam, Z. Kuang, P. Y. Craig, Y. Guo, H. Song, Q. Guo, J. M. Chan and A. Xia, *Phys. Chem. Chem. Phys.*, 2019, **21**, 17323-17331.
27. https://www.coherent.com/lasers/laser/astrella-ultrafast-tisapphire-amplifier.
28. https://www.coherent.com/lasers/laser/opera-solo-ultrafast-optical-parametric-amplifier.
29. https://ultrafastsystems.com/products/helios-fire.
30. J. J. Snellenburg, S. Laptenok, R. Seger, K. M. Mullen and I. H. M. van Stokkum, *Journal of Statistical Software*, 2012, **49**, 1 - 22.
31. A. L. Jones and K. S. Schanze, *J. Phys. Chem. A*, 2020, **124**, 7001-7013.
32. M. E. Köse and K. S. Schanze, *J. Phys. Chem. A*, 2020, **124**, 9478-9486.
33. H. Zheng, Y. Zhao, M.-X. Song, J. Wang, L.-Q. Chen, L. Sun and F.-Q. Bai, *Spectrochimica Acta Part A: Molecular and Biomolecular Spectroscopy*, 2018, **199**, 260-270.
34. F. Feng, J. Yang, D. Xie, T. D. McCarley and K. S. Schanze, *J. Phys. Chem. Lett.*, 2013, **4**, 1410-1414.
35. E. M. Kosower, *Acc. Chem. Res.*, 1982, **15**, 259-266.
36. N. Mataga, Y. Kaifu and M. Koizumi, *Bull. Chem. Soc. Jpn.*, 1956, **29**, 465-470.
37. A. L. Jones, M. K. Gish, C. J. Zeman IV, J. M. Papanikolas and K. S. Schanze, *J. Phys. Chem. A*, 2017, **121**, 9579-9588.
38. M. K. Gish, A. L. Jones, J. M. Papanikolas and K. S. Schanze, *J. Phys. Chem. C*, 2018, **122**, 18802-18808.
39. A. L. Jones and K. S. Schanze, *J. Phys. Chem. A*, 2019, **124**, 21-29.
40. J. Wan, A. Ferreira, W. Xia, C. H. Chow, K. Takechi, P. V. Kamat, G. Jones II and V. I. Vullev, *J. Photochem. Photobiol. A*, 2008, **197**, 364-374.
41. K. Matsumoto, M. Fujitsuka, T. Sato, S. Onodera and O. Ito, *J. Phys. Chem. B*, 2000, **104**, 11632-11638.
42. In some cases the Global kinetic fitting required four components to achieve convergence of the fitting routine. This process gives rise to two spectral components that are substantially similar (e.g., Fig. 4b and 4d). We do not attribute these to different excited states, rather they are due to a non-exponential relaxation in the spectral component that could be due to competing relaxation processes.

43. Y. Gong, X. Guo, S. Wang, H. Su, A. Xia, Q. He and F. Bai, *J. Phys. Chem. A*, 2007, **111**, 5806-5812.
44. Y.-J. Cho, A.-R. Lee, S.-Y. Kim, M. Cho, W.-S. Han, H.-J. Son, D. W. Cho and S. O. Kang, *Phys. Chem. Chem. Phys.*, 2016, **18**, 22921-22928.
45. J. Pina, J. S. de Melo, D. Breusov and U. Scherf, *Phys. Chem. Chem. Phys.*, 2013, **15**, 15204-15213.
46. E. Campioli, S. Sanyal, A. Marcelli, M. Di Donato, M. Blanchard-Desce, O. Mongin, A. Painelli and F. Terenziani, *ChemPhysChem*, 2019, **20**, 2860-2873.
47. A. Weller, 1982, **133**, 93-98.
48. J. Kroon, H. Oevering, J. W. Verhoeven, J. M. Warman, A. M. Oliver and M. N. Paddon-Row, *The Journal of Physical Chemistry*, 1993, **97**, 5065-5069.
49. H. Oevering, M. N. Paddon-Row, M. Heppener, A. M. Oliver, E. Cotsaris, J. W. Verhoeven and N. S. Hush, *J. Am. Chem. Soc.*, 1987, **109**, 3258-3269.